Bulk and surface magnetoplasmon modes of Cantor-type superlattices

1993 J. Phys.: Condens. Matter 5 4623

(http://iopscience.iop.org/0953-8984/5/27/007)

J. Phys.: Condens. Matter 5 (1993) 4623–4630. Printed in the UK

Bulk and surface magnetoplasmon modes of Cantor-type superlattices

Nian-hua Liu†, Wei-guo Feng‡ and Xiang Wu‡

† Pohl Institute of Solid State Physics, Tongji University, Shanghai 200092, People's Republic of China and Department of Physics, Jian Teachers Training College, Jian, Jiangxi 343009, People's Republic of China

‡ CCAST (World Laboratory), PO Box 8730, Beijing, 100080, People's Republic of China and Pohl Institute of Solid State Physics, Tongji University, Shanghai 200092, People's Republic of China

Received 4 January 1993, in final form 29 March 1993

Abstract. The bulk and surface magnetoplasmon modes of a Cantor-type superlattice, in which the cells consist of two alternating materials with their thicknesses following the Cantor sequence, are studied in the static approximation. The dispersion relations of the modes are presented concisely in terms of the transfer matrix elements. We find that the modes have fractal structure due to the special geometry of the superlattice. As a result of lowering the symmetry by applying an external magnetic field, the propagations of the surface magnetoplasmon become non-reciprocal. By plotting the profiles of the scalar potential amplititudes, we have also investigated the localization properties of the modes.

1. Introduction

The advances in crystal-growth techniques make it possible to tailor intentionally semiconductors or other materials to fabricate a new kind of artificial multilayered structure called a superlattice. The collective excitations of superlattices have in recent years attracted considerable interest. Much attention has been paid to the influence of the geometry of the superlattices on the plasmon modes because the modes depend critically upon the structure of the superlattices.

It is known that in superlattices, the surface excitations of individual layers coupled by the tails of the evanescent field give rise to the bulk modes propagating along the superlattice direction. For a simple periodic system, the bulk plasmon modes characterized by Bloch indices, and the surface modes supported by semi-infinite or finite superlattices, have been well investigated theoretically [1–5] and experimentally [6–9]. The influences of structures with different ratios of thicknesses of the alternating materials or with different dielectric constant designs on the plasmon modes were considered by Camley *et al* [1, 3]. The results shown that corresponding to different structures of the superlattices, there are very different plasmon modes. The interface charged sheets also affect the dispersion relations of the modes [4, 5]. With the removal of the translational symmetry of the superlattices, as in a superlattice with a non-regular layer [10], or a quasi-periodic region [11], some new interface plasmon modes appear. The symmetry can also be lowered by an external magnetic field [12, 13], which leads to the non-reciprocal propagation of the surface plasmons. Since Merlin *et al* succesfully grew a Fibonacci quasi-periodic superlattice, the collective excitations of the quasi-periodic heterostructures have been extensively studied.

0953-8984/93/274623+08$07.50

Hawrylak *et al* [15] have demonstrated that the bulk plasmon modes possess Cantor-like structure, and studied the scaling behaviours of the frequency spectrum. By taking account of retardation and spatial dispersion, Feng *et al* [16] have investigated the effects of the plasma waves on the optical properties of a Fibonacci superlattice. Theoretical work on the magnetoplasmons of the Fibonacci superlattice has been carried out by Johnson and Camley [17] and generalized by Albuquerque and Cottam [18].

The well known Cantor set is another interesting quasi-periodic system. In the study of the optical properties of Cantor-type superlattices, Wu *et al* [19] found that the optical reflection spectra and electromagnetic modes have well defined self-similar patterns and scaling behaviours. In particular, this fractal structure has very recently been used to study fractons [20], which have drawn increasing interest in the past few years. By constructing an artificial Cantor heterostructure and measuring the frequency spectra and amplitude of the vibration modes, Craciun *et al* found the direct evidence of the localized and self-similar character of the fractons.

In this work, we study the plasmon modes of the quasi-periodic Cantor-type superlattices in an external magnetic field applied parallel to the interfaces. The transfer matrix method has been employed, and the dispersion relations of the bulk and surface magnetoplasmon modes are presented implicitly in transfer matrix elements. We plot the profiles of the scalar potential amplitudes to investigate the localization of the modes. The numerical results show that the dispersion curves of the modes possess fractal structure due to the special geometry of the system. As a result of lowering the symmetry by the external magnetic field, the propagation of the surface magnetoplasmon has non-reciprocal properties.

2. General formalism of the dispersion relations

The system that we consider is a heterostructure consisting of a periodic array of unit cells alternating by two materials A and B. We let the thicknesses of the two constituent materials in a cell agree with the Cantor sequence (see figure 1), and take the z axis as the growth direction of the superlattice. The layer thicknesses are so large that the quantization of the electronic states by the superlattice potential is negligible, and the properties of the layers can be described by macroscopic dielectric functions [13]. We assume that the external magnetic field is applied parallel to the y axis; thus the dielectric tensor for a given layer is

$$\epsilon_\mu = \begin{pmatrix} \epsilon_{1\mu} & 0 & -i\epsilon_{2\mu} \\ 0 & \epsilon_{3\mu} & 0 \\ i\epsilon_{2\mu} & 0 & \epsilon_{1\mu} \end{pmatrix} \tag{1}$$

where

$$\epsilon_{1\mu} = \epsilon_{\infty\mu}[1 + \omega_{P\mu}^2/(\omega_c^2 - \omega^2)] \tag{2}$$

$$\epsilon_{2\mu} = \epsilon_{\infty\mu}\omega_{P\mu}^2\omega_c/\omega(\omega_c^2 - \omega^2) \tag{3}$$

$$\epsilon_{3\mu} = \epsilon_{\infty\mu}(1 - \omega_{P\mu}^2/\omega^2) \tag{4}$$

$$\mu = A, B$$

with ω_c and $\omega_{P\mu}$ denoting respectively the cyclotron frequency and the plasma frequency of the relevant material, and the subcript ∞ referring to the background dielectric constant.

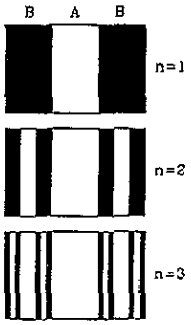

Figure 1. Three cells for the first-, second- and third-generation Cantor-type superlattices respectively.

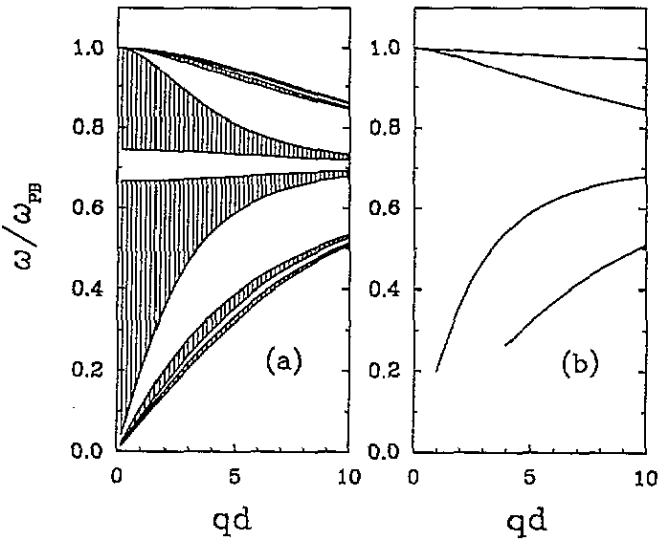

Figure 2. Dispersion curves of the plasmons for the second-generation Cantor-type superlattices: (*a*) bulk modes, and (*b*) surface modes.

Following Johnson *et al* [17], we take the static approximation and consider only the surface modes propagating along the x-axis direction. After solving Laplace's equation for a general layer, we can express the scalar potential as

$$\phi_l(x) = [A_l e^{-q(z-z_l)} + B_l e^{q(z-z_l)}]e^{i(qx-\omega t)} \qquad z_l < z < z_{l+1} \tag{5}$$

and the normal component of the electric displacement as

$$D_{zl}(x) = [qA_l(\epsilon_{1\mu} + \epsilon_{2\mu})e^{-q(z-z_l)} - qB_l(\epsilon_{1\mu} - \epsilon_{2\mu})e^{q(z-z_l)}]e^{i(qx-\omega t)} \qquad z_l < z < z_{l+1}. \tag{6}$$

The transfer matrix relationship of ϕ_l and D_{zl} connecting two different positions in the layer can then be established, that is

$$\begin{pmatrix} \phi_l \\ D_{zl} \end{pmatrix}_{z+\Delta z} = \mathbf{M}_\mu(\Delta z) \begin{pmatrix} \phi_l \\ D_{zl} \end{pmatrix}_z \tag{7}$$

where

$$\mathbf{M}_\mu(\Delta z) = \begin{pmatrix} \cosh q\Delta z + (\epsilon_{2\mu}/\epsilon_{1\mu}) \sinh q\Delta z & -(1/q\epsilon_{1\mu}) \sinh q\Delta z \\ -q\epsilon_{1\mu}(1 - \epsilon_{2\mu}^2/\epsilon_{1\mu}^2) \sinh q\Delta z & \cosh q\Delta z - (\epsilon_{2\mu}/\epsilon_{1\mu}) \sinh q\Delta z \end{pmatrix}. \tag{8}$$

The continuity of ϕ and D_z across the interfaces enables us to connect any two positions in the superlattice by a product of matrices. Obviously, the relationship of ϕ and D_z across a cell is

$$\begin{pmatrix} \phi_N \\ D_{zN} \end{pmatrix}_{z_0+d} = \mathbf{X}_N \begin{pmatrix} \phi_1 \\ D_{z1} \end{pmatrix}_{z_0} \tag{9}$$

where d and N are the thickness and the total number of the layers in a cell respectively, and

$$\mathbf{X}_N = \prod_{j=1}^{N} \mathbf{M}_\mu(d_j) \tag{10}$$

is the product of matrices mapping the Cantor sequence. On the other hand, the Bloch theorem leads to

$$\begin{pmatrix} \phi_N \\ D_{z\,N} \end{pmatrix}_{z_0+d} = \mathrm{e}^{\mathrm{i}pd} \begin{pmatrix} \phi_1 \\ D_{z\,1} \end{pmatrix}_{z_0}. \tag{11}$$

The combination of equation (9) with (11) results in the dispersion relation of the bulk modes as

$$\cos(pd) = \eta \qquad \eta \equiv \tfrac{1}{2}\mathrm{Tr}\,\mathbf{X}_N \tag{12}$$

and the allowed modes are determined by the condition of $|\eta| < 1$.

In order to find the dispersion relation of the surface modes, we consider a semi-infinite superlattice occupying the half-space of $z > z_0 = 0$. The Bloch index in equation (11) should now be replaced by a complex number

$$p = p_1 + \mathrm{i}p_2 \tag{13}$$

where the real part p_1 stands for the bulk modes propagating along the z-axis direction, and the imaginary part p_2 for the surface modes, and satisfies

$$p_2 = d^{-1}\ln(|\eta| + (\eta^2 - 1)^{1/2}) \qquad |\eta| > 1. \tag{14}$$

In the region of $z < 0$, the convergent solution of the scalar potential must be chosen. After matching the boundary conditions at the surface, we obtain the dispersion relation of the surface modes

$$|q|x_{12} - x_{11} + \gamma_\pm = 0 \tag{15}$$

where x_{ij} are the elements of the matrix $\mathbf{X}_N$, and $\gamma_\pm = \pm\mathrm{e}^{-p_2 d}$; here the sign is the same as that of η.

3. Numerical results and conclusions

In this section we present some numerical examples of the dispersion relations developed in the previous section. The model system is a GaAs superlattice with only B layers doped; thus the plasma frequency of A layers, $\omega_{\mathrm{P\,A}} = 0$. The background dielectric constants are taken as $\epsilon_{\infty\,\mathrm{A}} = \epsilon_{\infty\,\mathrm{B}} = 13.13$, and the half-space of $z < 0$ is assumed to be a vacuum.

Let us first examine the case without an external magnetic field. The bulk and surface modes for the generation number $n = 2$ are shown in figure 2. From the figure we see that there are two kinds of mode around the surface plasma frequency of the bulk material $\omega_{\mathrm{S\,B}} \equiv \omega_{\mathrm{P\,B}}/\sqrt{2}$: the high-frequency modes, which are higher than $\omega_{\mathrm{S\,B}}$, and the low-frequency modes, which are lower. The surface modes, as we have seen, are very close to

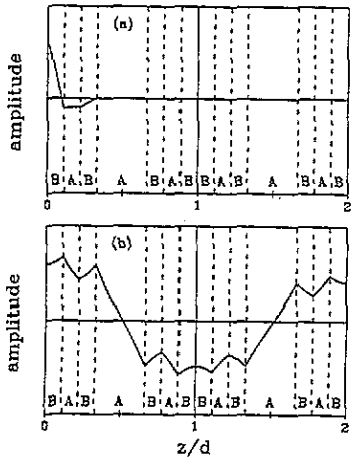

Figure 3. Amplitude of the scalar potential as a function of depth into the superlattice. Two unit cells for the generation number $n = 2$ are shown. The surface modes correspond to $qd = 5$; (a) for $\omega = 0.983\omega_{PB}$, and ($b$) for $\omega = 0.588\omega_{PB}$.

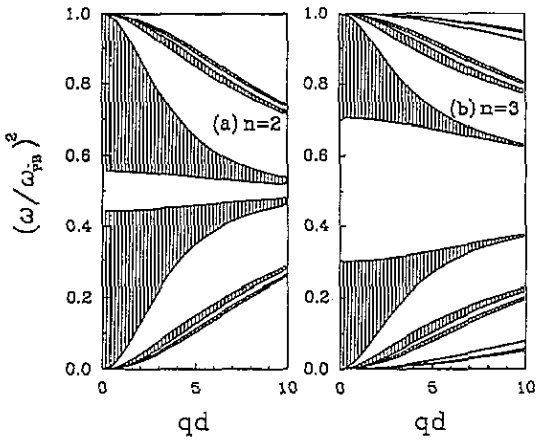

Figure 4. Dispersion curves of the square of the frequency versus the in-plane wavevector: (a) $n = 2$, (b) $n = 3$.

the bulk modes except for the uppermost one, and in the small-wavevector region, some surface modes embed into the bulk plasmon continuum. In figure 3, we have plotted the amplitude profiles: (a) $qd = 5$ with $\omega = 0.983\omega_{PB}$, and ($b$) $\omega = 0.588\omega_{PB}$. It is found that only the surface mode that is far from the bulk continuum is strongly localized at the surface (see figure 3(a)), while the surface mode that closes to the bulk continuum has very large penetrating depth (see figure 3(b)), it is very similar to the bulk modes near it (see figure 9(b)).

The total number of the bands of either high- or low-frequency bulk modes is identical to the number of gap layers in a cell (we refer to the undoped layer as a gap layer), that is

$$s_n = \sum_{k=0}^{n-1} 2^k \tag{16}$$

where n is the generation number. If we change the scale of the frequency axis to the square of frequency, as shown in figure 4, in which we have plotted the dispersion curves of the square of the frequency versus the in-plane wavevector for generation numbers $n = 2$ and $n = 3$, we find that the bulk modes have well defined reflection symmetry about $0.5\omega_{PB}^2 = \omega_{SB}^2$. With increasing generation number, the modes shift toward higher and lower frequencies. It can be seen that bulk modes consist of two groups for $n = 2$, and three groups for $n = 3$ in both high- and low-frequency regions, since there are two and three different gap layers' thicknesses in the cells for $n = 2$ and $n = 3$, respectively. The number of bands in each group is exactly equal to the number of relevant layers with the same thickness. For example, the three groups of bulk modes for $n = 3$ have respectively 1, 2 and 4 bands corresponding to three different gap thicknesses $d/3$, $d/3^2$ and $d/3^3$. In figure 5, we have plotted the dispersion relations of ω versus Bloch index p for $qd = 5$ to identify the bands that are too close to be resolved in the scale of figure 4. From the

figure, seven bands of low-frequency modes can clearly be seen. We believe that this kind of fractal structure of the modes is characteristic of the special geometry of the Cantor-type superlattice.

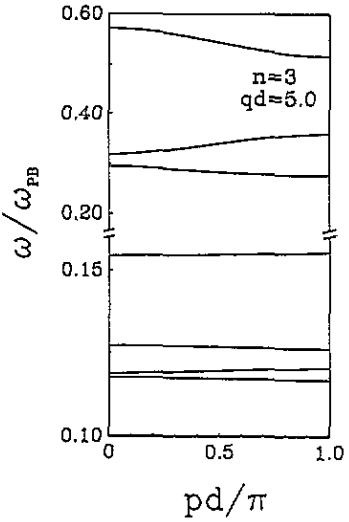

Figure 5. Dispersion curves of the frequency versus the Bloch index for $n = 2$ and $qd = 5$.

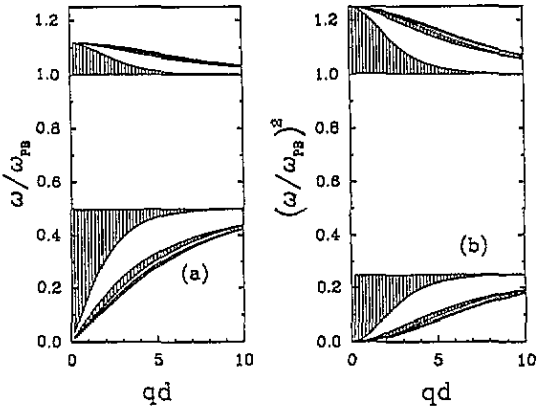

Figure 6. Dispersion curves of the bulk magnetoplasmon modes for $n = 2$ with the cyclotron frequency $\omega_c = 0.5\omega_{PB}$: (*a*) the frequency versus the in-plane wavevector; (*b*) the square of frequency versus the in-plane wavevector.

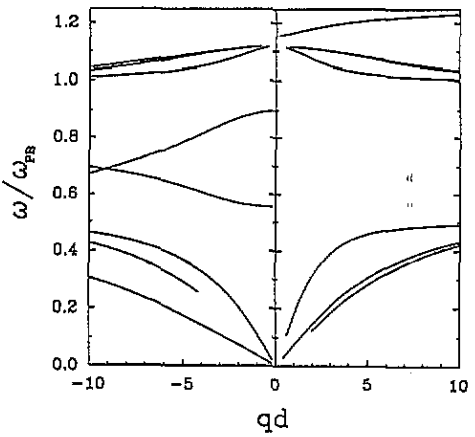

Figure 7. The non-reciprocal dispersion curves of the surface magnetoplasmon modes: the relevant parameters are the same as in figure 6.

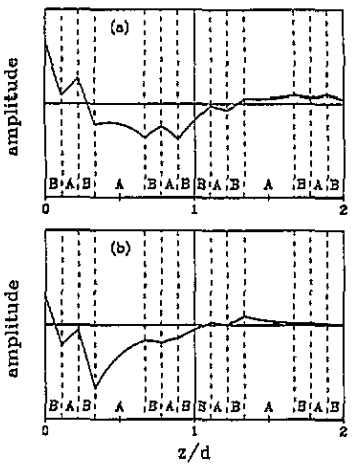

Figure 8. Amplitude profiles of two surface magnetoplasmon modes, (*a*) $qd = 5$ and $\omega = 1.02\omega_{PB}$, (*b*) $qd = -5$ and $\omega = 1.04\omega_{PB}$. The other relevant parameters are the same as in figure 6.

Now we turn to the investigation of the effects of the static external magnetic field on the plasmon modes. We assume that the magnetic field is applied so that the cyclotron frequency $\omega_c = 0.5\omega_{PB}$. The bulk magnetoplasmon modes for $n = 2$ are shown in figure 6; note that the scale of the frequency axis in panel (b) is the square of the frequency. We have seen that the modes shift toward the higher- and lower-frequency regions, and the widths of the bands are narrowed by the applied magnetic field. The reflection symmetry in the scale of the square of the frequency still exists, but the symmetrical centre moves to the position $0.625\omega_{PB}^2$ from that of $0.5\omega_{PB}^2$ the case without external magnetic field.

As indicated in [12] and [17], the applied external magnetic field can lower the symmetry of the system and lead to non-reciprocal propagations of the surface magnetoplasmons, and it is therefore important for device application. In figure 7, we show the non-reciprocal dispersion relations of the surface modes. From the figure, we find that two branches of surface modes located in the frequency gap between the high- and the low-frequency bulk modes appear in the negative-wavevector region. The different localization characters of the non-reciprocal surface modes are shown in figure 8, in which two amplitude profiles correspond to (a) $qd = 5$ with $\omega = 1.02\omega_{PB}$ and (b) $qd = -5$ with $\omega = 1.04\omega_{PB}$. We see from the figure that the mode depicted in panel (a) is mostly localized at the surface, but the mode in (b) is localized at the fourth interface.

Finally, we consider the influence of thickness or wavevector and the external magnetic field on the localization properties of the bulk modes. Four typical amplitude profiles of the bulk modes are shown in figure 9. The panels (a) and (b) are related to the modes at the edges of the uppermost band in the low-frequency region for $n = 2$ with $qd = 5$ and without the external magnetic field; a symmetry and an anti-symmetry mode can be seen in (a) and (b) respectively. When we increase the value of qd, which means increasinge the thickness d or wavevector q, the modes are more localized at the interface, as shown in (c), in which the mode corresponds to the symmetry state but $qd = 10$. The effect of applied magnetic field on the localization of the modes is shown in (d), in which the mode corresponds to the anti-symmetry state but with the cyclotron frequency $\omega_c = 0.5\omega_{PB}$; we observe that differing from (b), the mode is mostly localized at the second and fourth interfaces in the cells, which means that the magnetic field makes the modes further localized.

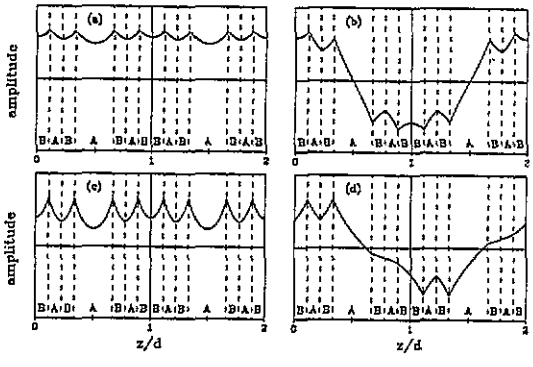

Figure 9. Amplitude profiles of four bulk plasmon modes for $n = 2$: (a) $qd = 5$, $\omega = 0.678\omega_{PB}$, and $\omega_c = 0$; (b) $qd = 5$, $\omega = 0.589\omega_{PB}$, and $\omega_c = 0$; (c) $qd = 10$, $\omega = 0.694\omega_{PB}$, and $\omega_c = 0$; (d) $qd = 5$, $\omega = 0.469\omega_{PB}$, and $\omega_c = 0.5\omega_{PB}$.

In conclusion, we have presented the dispersion relations of the bulk and surface plasmon modes of Cantor-type superlattices including the effects of the applied external magnetic field. As a result of the special geometry of the system, the fractal structure of the modes is found. By plotting the amplitude of the scalar potentials, we have investigated the

localization of the modes. We find that the modes are more localized in the external magnetic field. The non-reciprocal propagation caused by the external magnetic field is examined. As pointed out in [17], the non-reciprocal behaviours of the modes could be important for device applications. The bulk and surface plasmon, as we know, can be observed experimentally by, for example, inelastic light scattering [6–8], or far-infrared attenuated total reflection spectroscopy [9], or electron-energy-loss spectroscopy [21]. We hope that our theoretical results stimulate the interest of experimentalists.

Acknowledgments

We gratefully acknowledge useful conversations with Professors Yu-mei Zhang and Hong Chen. Part of this work was supported by the Chinese National Advanced Technology Foundation through grant 040–144–05–085.

References

[1] Camley R E and Mills D L 1984 *Phys. Rev.* B **29** 1695
[2] Giuliani G F and Quinn J J 1983 *Phys. Rev. Lett.* **51** 919
[3] Johnson B L, Weiler J T and Camley R E 1985 *Phys. Rev.* B **32** 6544
[4] Constantinou N C and Cottam M G 1986 *J. Phys. C: Solid State Phys.* **19** 739
[5] Farias G A, Auto M M and Albuquerque E L 1988 *Phys. Rev.* B **38** 12540
[6] Olego D, Pinczuk A, Gossard A C and Wiegmann W 1982 *Phys. Rev.* B **25** 7867
[7] Pinczuk A, Lamont M G and Gossard A C 1986 *Phys. Rev. Lett.* **56** 2092
[8] Fasol G, Mestres N, Hughes H P, Fischer A and Ploog K 1986 *Phys. Rev. Lett.* **56** 2517
[9] Dumelow T, Parker T J, Tilley D R, Beall R B and Harris J J 1991 *Solid State Commun.* **77** 253
[10] Bloss W L 1991 *J. Appl. Phys.* **69** 3068; 1991 *Phys. Rev.* B **44** 1105
[11] Liu N, Feng W G and Wu X 1992 *J. Phys.: Condens. Matter* **4** 9823
[12] Johnson B L and Camley R E 1988 *Phys. Rev.* B **38** 3311
[13] Albuquerque E L, Fulco P, Farias G A, Auto M M and Tilley D R 1991 *Phys. Rev.* B **43** 2032
[14] Merlin R, Bajema K, Clarke R, Juang F Y and Bhattacharya P K 1985 *Phys. Rev. Lett.* **55** 1768
Todd J, Merlin R, Clarke R, Mohanty K M and Axe J D 1986 *Phys. Rev. Lett.* **57** 1157
[15] Hawrylak P and Quinn J J 1986 *Phys. Rev. Lett.* **57** 380
Hawrylak P, Eliasson G and Quinn J J 1987 *Phys. Rev.* B **36** 6501
[16] Feng W G, Liu N and Wu X 1991 *Phys. Rev.* B **43** 6893
[17] Johnson B L and Camley R E 1991 *Phys. Rev.* B **44** 1225
[18] Albuquerque E L and Cottam 1992 *Solid State Commun.* **81** 383
[19] Wu X, Yao H S and Feng W G 1991 *SPIE* vol 1519, (Bellingham, WA: SPIE) p 625
Feng W G, Liu N and Wu X *SPIE* vol 1928, to be published
[20] Craciun F, Bettucci A, Molinari E, Petri A and Alippi A 1992 *Phys. Rev. Lett.* **68** 1555
[21] Rocca M, Lazzarino M and Valbusa U 1992 *Phys. Rev. Lett.* **69** 2122